JOURNAL OF MECHANICS OF CONTINUA AND MATHEMATICAL SCIENCES
www.journalimcms.org

ISSN (Online) : 2454 -7190 Vol.-16, No.-7, July (2021) pp 32-56 ISSN (Print) 0973-8975

PERFORMANCE EVALUATION OF VOLTAGE RECTIFIERS FOR ENERGY HARVESTING APPLICATIONS

Atif Sardar Khan[1], Nasir Ullah Khan[2], Wahad Ur Rahman[3]
Muhammad Masood Ahmad[4], Hamid Khan[5], Farid Ullah Khan[6]

[1,2,3,5,6]Department of Mechatronics, University of Engineering and Technology Peshawar, Pakistan.

[4]Department of Mechanical, University of Engineering and Technology Peshawar, Pakistan.

[1]atifsardarkhan@uetpeshawar.edu.pk, [2]engrnasir_ullah@outlook.com,
[3]wahadurrahman@uetpeshawar.edu.pk, [4]masood@uetpeshawar.edu.pk,
[5]engrhamidkhan@gmail.com, [6]dr_farid_khan@uetpeshawar.edu.pk

Corresponding Author: **Atif Sardar Khan**

https://doi.org/10.26782/jmcms.2021.07.00004

(Received: May 8, 2021; Accepted: July 3, 2021)

Abstract

Voltage multipliers are used to convert the low AC voltage output of energy harvesters into relatively high DC voltage for portable devices and wireless sensor nodes (WSNs) applications. DC voltage conversion is required to operate an electronic device or recharge a battery. In order, to convert the low AC voltage output of the energy harvester into relatively high DC voltage, a voltage multiplier circuit need to be integrated with the energy harvester. In this study, Prototype-1 (two-stages) and Prototype-2 (three-stage) Dickson voltage multipliers and Prototype-3 (seven-stage) Cockcroft-Walton voltage multiplier circuits are developed. The device is capable of converting a low voltage of 50 mV into 350 mV. The research focuses on the development and characterization of Prototype-1, Prototype-2 and Prototype-3 circuits. Results indicate that the determination of load resistance is important for better output power. The maximum power of 11.97 μW was obtained by prototype-3 elucidating better power compared to prototype-1 and prototype-2 and the power was obtained at an optimum load of 560 kΩ. Furthermore, a rectenna tested at different distances from the source, revealed that prototype-2 produced a maximum power of 3.01 × 10 -6 μW, at an optimum load of 560 kΩ.

Keywords: Voltage multipliers, energy harvesters, AC to DC, rectifier, low voltage, flow-based, RF,

I. Introduction

The rapid advancements in wireless sensor technology [VII], internet of things [VIII] and energy harvesting [XV, XXI] made ways for the development of integrated autonomous systems. Vibration-based [XXII, IX, I] and acoustic-based [X] energy harvesters are successfully developed to power the integrated sensors. In these harvesters electromagnetic [II] and piezoelectric [XXIV] mechanisms are adopted for energy transduction. Moreover, the notion of a widely interconnected, adaptive, and dynamic ubiquitous computing environment has been proposed for decades [XXXIX]. Recently the wireless sensor networks (WSNs) technology got recognition for the emerging pervasive computing areas [XXXI]. Due to the rapid growth, wireless sensor networks (WSNs) have a wide range of applications ranging from civil and military to environmental monitoring, home automation, surveillance, precision agriculture, machine fault diagnosis, inventory control, and biomedical applications [III]. Over the years, researchers have focused on low power and efficient techniques at the physical layer, medium access, and routing layers, but even then, the battery drainage with the most efficient sensing and communication protocol is not impressive to operate the sensor nodes and keep the WSNs active for a longer period [XXIII]. The use of WSNs is limited by the constraint of limited battery's power. Replacement and charging of batteries in hard and far flange areas, like desert and deep-ocean are costly and unfeasible.

Therefore, energy-harvesting techniques to extract ambient energy sources are used to prolong the life of the batteries in WSNs [XXXIV]. The energy sources available in an environment are vibration, acoustic, thermal, wind and tidal. Moreover, radiofrequency (RF) signals are also abundantly present in the surroundings. RF signals radiated by broadcasting stations and cellular phone antennas can be scavenged through a rectenna (RF energy harvester). However, the power generated by the RF energy harvester is in nW range and even for μW power production, the maximum efficiency achieved is 20 % [XVII]. Likewise, sound energy is present almost everywhere in the environment, for example, the telephone dial tone is 80 dB, a train whistle is 90 dB, jet engine (140 dB) and aircraft produces 194 dB which are adequate sound pressure levels (SPLs) that can be used for energy harvesting [XXVIII]. Techniques for the conversion of vibration energy into electrical energy include, electrostatic, piezoelectric and electromagnetic. Typical efficiencies for these energy transductions are 0.32% for electrostatic [XXVI]; 0.5% (PVDF) to 20% (PZT) for piezoelectric [XXXII]; and 6% for electromagnetic [XXVI].

An alternating current (AC) output voltage signal produced by most of the energy harvesters [XXXII] is in few mV to few V, however, for sensor and portable electronic the demand of DC voltage from 2 to 12 V for operation is required. The production of relatively high DC voltage from low and ultra-low AC voltage is gaining rapid interest. Therefore, many attempts have been made to discover ways to generate DC voltage higher than the supply AC voltage of the energy harvester. Some of the most commonly applied methods for high DC voltage generation than the low supply AC voltage, include step-up transformers [XXXII], voltage doubler [XXIX] [XVIII], switched-capacitor circuits [XXV][VI], and boost or step-up converters [XIX, XXXV,

IV, XXXVIII]. However, among these methods, diode-capacitor topologies are more suitable.

II. Literature Review

A low-voltage four-quadrant analog multiplier using dynamic threshold Metal Oxide Semiconductor Field Effect Transistor (MOSFET) transistor (DTMOS) [XXXVI] circuit topology was developed for an application of an analog VLSI library cell since the circuit complexity and supply voltage requirements are low. It can even work at a low AC supply voltage of 0.5 V and achieves high linearity and an extended frequency range of 250 MHz.

An AC-DC converter [XI] was produced as an application for energy harvesting. The developed circuit is fabricated using TSMC 130 nm CMOS technology with an active area of 0.249 mm^2. In the circuit, the active diode included a positive metal oxide semiconductors (PMOS) switch controlled by a comparator. The input AC voltage levels range from 0.5 to 4 V at 40-150 Hz were rectified to a DC voltage in the range from 0.8 to 12 V with a maximum power efficiency of 71% achieved for the input AC amplitude of 1.5 V. An ultra-low-power (ULP) diode is connected to Villard and Dickson voltage multiplier instead of diode connected to a PMOS is developed [XXXX]. By usage of ULP diode, the performance of the circuit improved, as the leakage current decreased and relatively much higher output DC voltage is produced compared to diode-connected PMOS diode. Due to the ULP diode in the Dickson rectifier, the efficiency increased from 8.19% to 17.74% is reported. Moreover, the Dickson rectifier was also considered as a high sensitivity rectifier since it can produce 0.214 V with an input AC voltage of 0.2 V and 3.54 with an input AC voltage of 1 V. A 0.18-V input three-stage charge pump circuit is designed and fabricated [XXXIII] specifically for low voltage applications. The developed circuit based on voltage doubler is fabricated using 65 nm standard CMOS technology. All the MOSFETs are forward body biased by using the inter-stage/output voltages. By applying the proposed charge pump as the start-up in the boost converter, the lower kick-up input voltage of the boost converter can be achieved. The output voltage is boosted from 0.18 V input to 0.74 V under 6 mA output current. A 7-stage Cockcroft-Walton voltage multiplier was designed and fabricated [XII] to capture RF power for the application of battery charging. The prototype is fabricated on RT/ Duroid 5880 (RO5880) printed circuit board (PCB) substrate with dielectric constant and loss tangent of 2.2 and 0.0009 respectively. The output voltage is found to be 6.47 V harvested from the RF signal operating at a frequency of 900 MHz. Villard voltage doubler rectifier [XX] was developed for RF energy harvesting system at 900 MHz band. RF signals are converted into direct-current (DC) voltage at the given frequency band to power the low power devices and circuits. A 7-stage Schottky diode voltage doubler circuit was able to produce 3 mV across a 100 kΩ load for an equivalent incident signal of –40 dBm. Moreover, it is reported that the output voltage reaches 1.0 V within 20 μs and then increases to 1.4 V, 1.67 V, 1.87 V and 2.12 V for 4, 5, 6 and 7 stages respectively. A 3-

stage voltage doubler [XIII] is developed for charging mobile applications. A 3-stage voltage doubler is an impedance matched to a 900 MHz band antenna. The Antenna and rectifier are modeled and optimized using the Agilent Advanced design system (ADS) 2009. The output voltage of the rectifier is 5.014 V for a 3-stage voltage doubler after the matching circuit is included. A 7-stage doubler circuit [XXVIII] was developed for an antenna operating at 900 MHz to run an STLM20 temperature sensor. The antenna has a partial ground plane in the structure to maximize the energy captured and generating higher DC output voltage levels. A 7-stage doubler circuit was optimized using ADS. All three modules were integrated and fabricated on a double-sided FR4 printed circuit board. The output voltage harvested from the rectenna at a distance of 50 m from the GSM cell tower was 2.9 V. A 7-stage Cockcroft-Walton rectifier was developed for the application of low RF power energy harvesting [XXX] to power the radio frequency identification (RFID) tags. Moreover, a rectenna with a matching circuit was also reported. The Prototype was fabricated on RT/Duroid 5880 (RO5880) printed circuit board (PCB) substrate with dielectric constant and loss tangent of 2.2 and 0.0009 respectively. The output voltage of 1.5 V was harvested at a frequency of 2.48 GHz with 0.1 mW input power.

III. Working Principle of Voltage Multiplier

To multiply the input voltage, voltage multipliers are required. There are three types of voltage multiplier which are Cockcroft-Walton, Dickson and Greinacher voltage multiplier.

Voltage multipliers consist of Schottky diodes and capacitors. HSMS- 2852 Schottky diodes are used in this work which has low forward voltage, an advantage of low junction capacitance and fast switching speed.

Cockcroft-Walton Voltage Multiplier

An AC voltage input is converted into a DC voltage by a multiplier circuit. As shown in figure 1, where figure 1(a) and figure 1(b) are the voltage multiplier operations in the negative half cycle, whereas, figure 1(c) and figure 1(d) are working of the circuit during the positive half cycle. The capacitor, C_1 charges through the diode, D_1 as shown in figure 1(a) in a negative half cycle which leads the capacitor to be positive at its right side and negative at its left. In figure 1(b) the positive half cycle voltage adds to C_1, which was charged in the negative half cycle. Therefore, capacitor, C_2 charges through D_2 to $2V_s$. In figure 1(c), the charge stored in C_1 was used in the previous cycle, so C_1 is now charging through D_1. Also, capacitor, C_3 is charged through D_3 to $2V_s$. While in figure 1(d), for the positive half cycle, C_2 is recharged. Just like the negative half cycle this time, capacitor, C_4 charges to $2V_s$. The Capacitors charges fully until several cycles are passed, depending on the charging current.

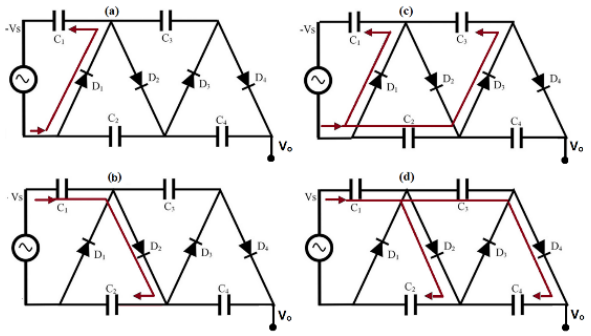

Figure 1. Working principle of the two-stage voltage multiplier: (a) negative half cycle of the first stage, (b) positive half cycle for the first stage, (c) negative half cycle for the second stage, (d) positive half cycle for the second stage.

Villard voltage multiplier is also known as Cockcroft-Walton voltage multipliers [XIV], is shown in Figure 1. The output of the n-stage Villard voltage multiplier is given in (1)

$$V_{DC} = \frac{nVo}{nR_o + R_L} \tag{1}$$

Where, V_0 is an open circuit output voltage for a single-stage and R_0 is the internal resistance of the single-stage and R_L is the load resistance.

Dickson Voltage multiplier

Dickson voltage multiplier (n-stages) is shown in figure 3, the parallel configuration of capacitors in each stage reduces the circuit impedance, and hence makes the matching task simpler [XXVIII] when compared with Cockcroft-Walton voltage multipliers.

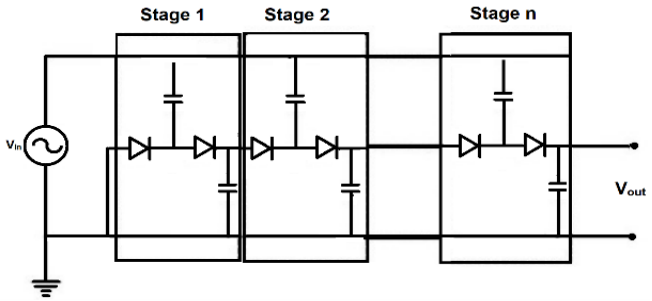

Figure 2. N-stage Dickson Voltage Multiplier

The output voltage of the n-stage Dickson voltage multiplier is given by (2) [XXV].

$$V_{DC} = n\,(V_m - V_T) \tag{2}$$

where n is the number of stages, V_m is the peak amplitude of the input voltage and V_T is the forward conduction voltage of the diodes.

Greinacher Voltage Multiplier

Greinacher voltage multiplier circuit as shown in figure 4, where capacitor C1 and diode D1 shift the input voltage up at node A to be rectified by diode D2. Capacitor C3 and diode D3 shift the voltage down at node B to be rectified by diode D4 and capacitor C4. After reaching balance, the circuit provides a constant output current and voltage to the load [II]. The output voltage of the Greinacher voltage multiplier is given by (3) [XXIX]

$$V_{DC} = 2nV_m \tag{3}$$

where n is the number of stages and V_m represents the peak amplitude of an input voltage.

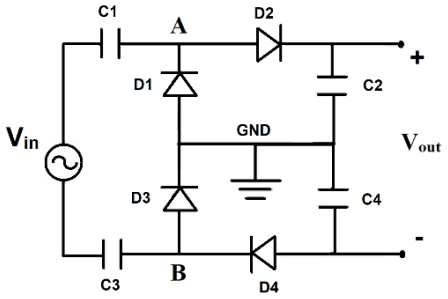

Figure 3. The basic circuit of the Greinacher Voltage Multiplier

The objective of this research is to develop a rectifier for energy harvester for applications. Four rectifying circuit prototypes are fabricated and characterized for performance evaluation. Two different types of Schottky diodes are used to evaluate their performance. Furthermore, all three rectifying circuit prototypes are integrated into a 2.45 GHz antenna, where prototype-3 couldn't operate due to seven stages causing power losses. So the experimentation concludes that stages of rectifying circuit should be one or two otherwise, the rectifying circuit may not perform as reported in this work.

IV. Fabrication of Voltage Multiplier Circuits

Fabrication of prototype-1

The circuit diagram of a developed Prototype-1 is shown in figure 2. A low and ultra-low voltage conversion Schottky diodes (HSMS–2852) are used for the development of Prototype-1. Moreover, surface-mounted capacitors are used in the development of this prototype, which is connected with diodes on a printed circuit board (PCB) FR-4 substrate**.** Table 2 shows the circuit elements for the development of Prototype-1. For the PCB development of the voltage multiplier circuits, an ADS 2017 is utilized to produce a circuit layout. After that, the circuit is printed on FR-4 PCB substrate of 4.57 x 7.62 cm^2 with dielectric constant and loss tangent of 4.3 and 0.02 respectively. After that, the soldering of components on the FR-4 sheet was done by using SMT Rework station at 180 °C.

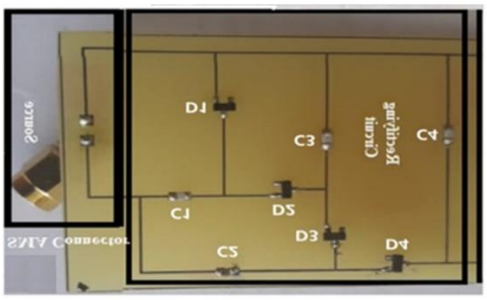

Figure 4. Developed Dickson type two stages voltage multiplier circuit (prototype-1)

Fabrication of prototype 2

Figure 3 shows the photograph of the developed prototype 2. This is a three-stage Dickson-type voltage multiplier circuit. An ultra-low-voltage SMD type Schottky diodes (HSMS – 2852) are used in the development of Prototype-2. Moreover, surface-mounted capacitors of 100 pF are connected with diodes on PCB FR-4 substrate. Similar to prototype-1 for the PCB development, an ADS 2017 was utilized to produce a circuit layout of prototype-2. After that, An FR-4 PCB substrate of 4.57 x 7.62 cm^2 with dielectric constant and loss tangent of 4.3 and 0.02 respectively are used for the development of the circuit. The last soldering of components on the FR-4 sheet was done by using SMT Rework station at 180 °C.

Figure 5. Developed Dickson type three stages Voltage multiplier circuit (Prototype-2)

Fabrication of prototype-3

A Cockcroft-Walton type seven stages voltage multiplier circuit is developed in figure 5. For the development of prototype 3, an ultra-low voltage SMD type Schottky diode (HSMS-285 C) and 1000 pF of capacitors are used. Prototype-3 is fabricated using photographic paper for circuit printing through a laser inkjet printer. The PCB sheet was cleansed with sandpaper for the removal of the copper oxide layer. Then, the PCB on which the circuit had to be printed was washed with distilled water and dried in compressed air. The pattern transferring was done by keeping an electric iron on the photographic paper for ten minutes. After that, an etching was done by dissolving the Ferric Chloride in warm water and the solution of ferric chloride and a copper-clad sheet with a circuit pattern was stirred for 10 minutes. The circuit layout pattern was

patterned and erased with sandpaper for revealing copper traces on the PCB. Finally, the components were soldered on the developed PCB.

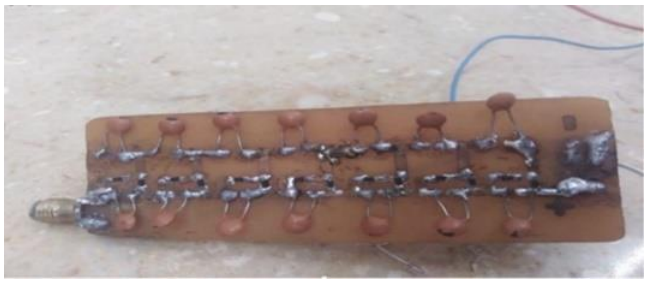

Figure 6. Developed Cockcroft Walton type seven stages Voltage multiplier circuit (prototype-3)

Fabrication of prototype-4

A three-stage Cockcroft Walton type (Figure 7) AC to DC voltage rectification circuits is developed for converting the low AC output of flow-based energy harvester into higher DC voltage for powering the WSN used in the pipeline monitoring system. This type of rectifying circuit will not only convert the AC output of the harvester into DC voltage but also step up the voltage due to its multi-stages. For low voltage drop across the circuit, a low voltage surface mount Schottky diode (SS34 1N588 SMA DO-214AC) is selected. Moreover, 330 µF, 25 V surface mount capacitors are utilized to be connected with these diodes. The prototype was developed on a Vero circuit board using fine soldering techniques.

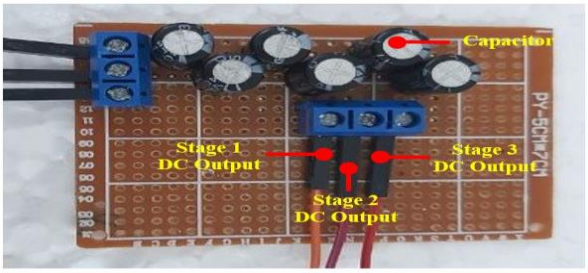

(a)

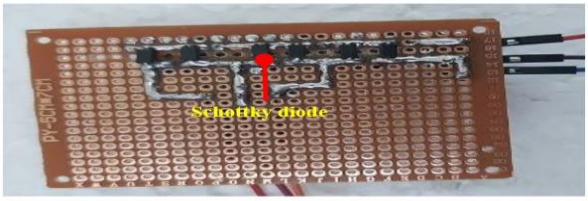

(b)

Figure 7. Developed Cockcroft Walton type three stages voltage multiplier circuit (prototype 4): (a) Front view, (b) Back view

Table.1 Main Parts of prototypes

Prototypes	Topology	Stages	Schottky diodes	Capacitor (pF)	Board type	Substrate
Prototype-1	Dickson	Two	HSMS – 2852	C1,C2 = 5 C3 =15	PCB	FR-4
Prototype-2	Dickson	Three	HSMS 285-C	100	Stripboard Circuit Board	FR-4
Prototype-3	Cockcroft Walton	Seven	HSMS 285-C	1000	Stripboard Circuit Board	FR-4
Prototype-4	Cockcroft Walton	Three	SS34 1N588	330000	Vero Circuit Board	-

V. Results and Discussion

Characterization of prototype-1

Figure 8 shows the in-lab experimental testing setup for the characterization of prototype-1, prototype-2 and prototype-3. The function generator used in the experimental setup is utilized to generate a variable AC voltage signal at different frequencies. A multimeter and oscilloscope were used to measure the input and output voltages of developed prototype circuits. The voltage across the voltage multiplier circuit was measured through the variable load for an optimum load and maximum power.

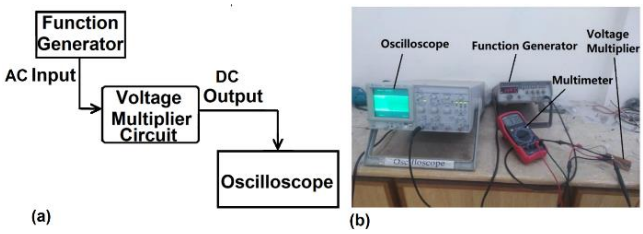

Figure 8. Experimental setup for the testing of voltage multiplier circuits (a) Block diagram (b) Actual Experimental setup.

Figure 9 shows an open circuit voltage produced by prototype 1 as a function of input signal frequency. The amplitude of the input signal generated by the function generator was varied from 75 mV to 1500 mV for the frequency range of 100 kHz to 1.5 MHz. An output open circuit DC voltage at the rectifier output was measured with the help of an oscilloscope and digital multimeter. An output DC voltage of 22 mV to 1862 mV is obtained for prototype 1.

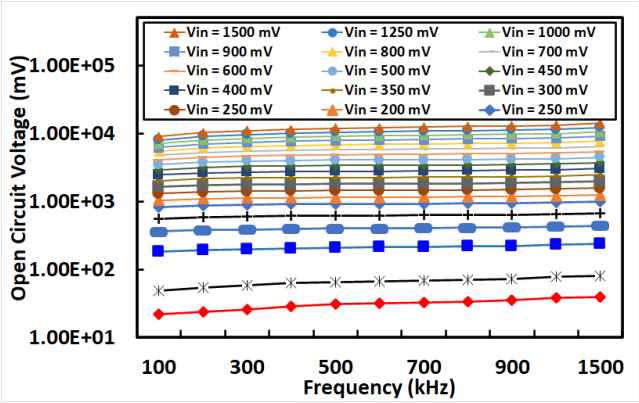

Figure 9. Output open circuit DC voltage versus input AC voltage frequency (prototype-1)

Figure 10 shows an open circuit output DC voltage in response to the input AC voltage produced by prototype-1. An input signal amplitude is varied from input 1.1 mV to 1500 mV and their corresponding DC voltage is measured. It is cleared from the figure an input AC voltage of 50 mV is converted into 205 mV DC and the maximum voltage prototype 1 achieved is 1.25 V.

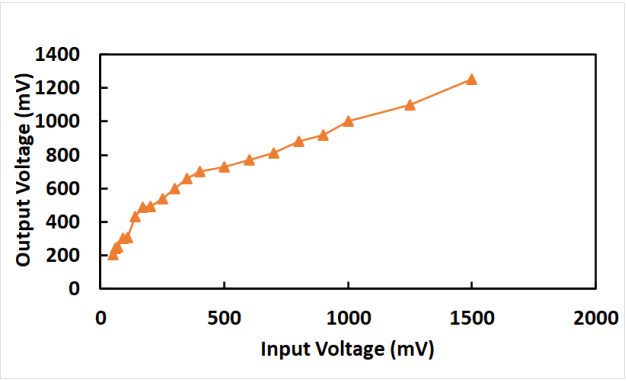

Figure 10. Output DC voltage as a function of input AC voltage for (prototype 1)

Output load DC voltage produced by prototype 1 as a function of load resistance for the different input voltage is shown in figure 11. During experimentation, for an input voltage range from 50 mV to1500 mV, various resistors were connected and the voltage across each resistor was recorded. It is cleared from figure 11 that the output voltage increases as the load resistance is changed from a lower value to a higher value.

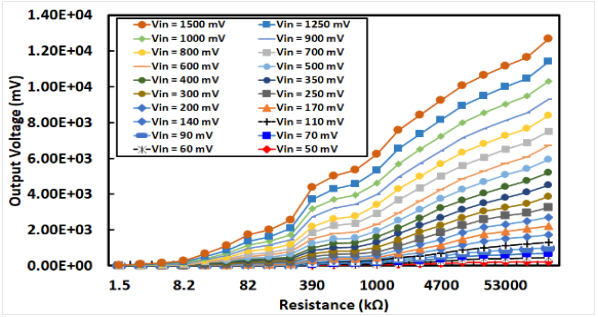

Figure 11. Output load voltage versus load resistance (prototype-1)

Output load Power produced by prototype-1 as a function of load resistance for the different input voltage is shown in figure 10. The characterization was performed under an input frequency of 1.5 MHz. The load resistance is varied from 1.5 kΩ to 60 MΩ and the corresponding load power is recorded. At optimum load resistance of 470 kΩ, a maximum load power of 1.1 µW is produced.

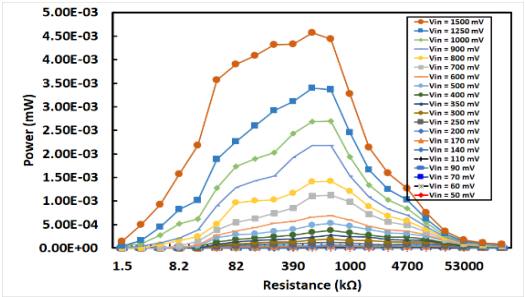

Figure 12. Load power as a function of load resistance (prototype-1)

The transformation factor (V output/V input) versus load resistance is shown in figure 13. The maximum transformation factor obtained is 4.1 for an input voltage of 50 mV. The least transformation factor obtained was 0.00016 for an input AC voltage of 600 mV at a load resistance of 1.5 kΩ.

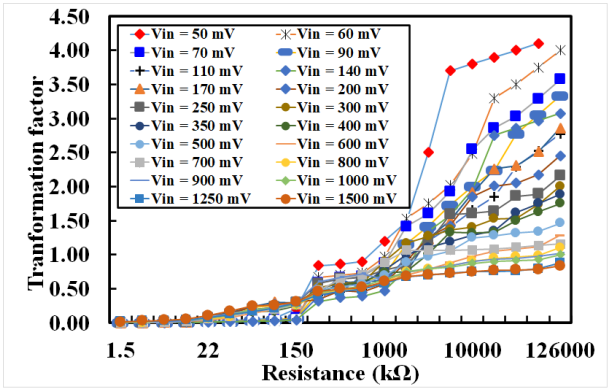

Figure 13. Transformation factor versus load resistance for prototype-1

Characterization of prototype-2

Prototype-2 is characterized inside the lab using the experimental setup developed in figure 8. Figure 14 shows an open circuit DC voltage produced by prototype 2 as a function of input signal frequency. The amplitude of the input signal generated by the function generator was varied from 75 mV to 1500 mV for the frequency range of 100 kHz to 1.5 MHz. An output open circuit DC voltage of 21.4 mV to 5690 mV is obtained at the rectifier output of prototype-2.

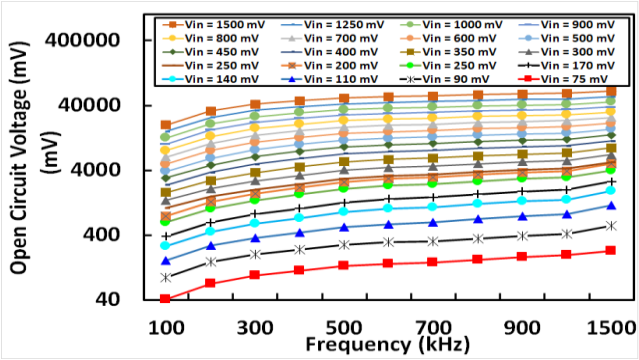

Figure 14. Output open circuit DC voltage versus input AC voltage frequency (prototype -2)

Open circuit DC voltage in response to the input AC voltage is analyzed in figure 15 for the developed prototype 2. An input signal amplitude is varied from input 1.1 mV to 1500 mV and their corresponding DC voltage is measured. It is cleared from the figure an input AC voltage of 50 mV is converted into 350 mV DC and the maximum output voltage DC voltage produced is 5.4 V.

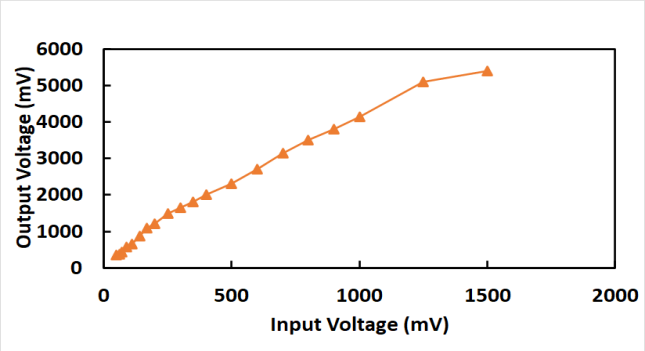

Figure 15. Output DC voltage as a function of input AC voltage for prototype-2

In this experimentation, an output load DC voltage produced by the developed prototype-2 as a function of external load resistance for different input voltage is shown in figure 16. During this experimentation, various load resistors were connected with the rectifier output and their corresponding voltage is measured.

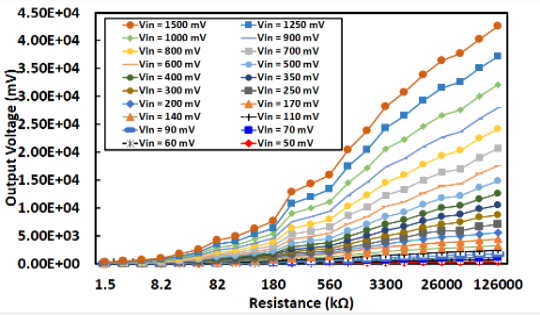

Figure 16. Output load voltage versus load resistance (prototype-2)

Figure 17 shows the Output load Power produced by prototype 2 as a function of external load resistance for different input voltages. The characterization was performed under an input frequency of 1.5 MHz. The load resistance is varied from 1.5 kΩ to 60 MΩ and the corresponding load power is recorded. At optimum load resistance of 560 kΩ, a maximum load power of 11.97 µW is produced.

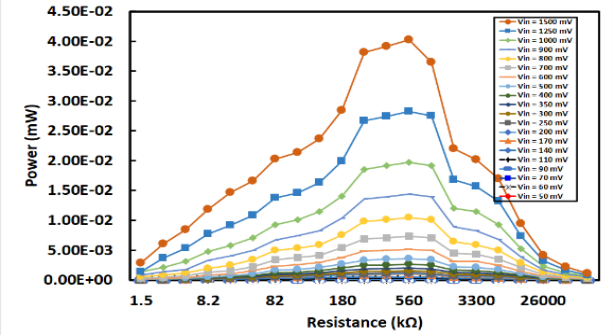

Figure 17. Load power as a function of load resistance (prototype-2)

The transformation factor (V output/V input) versus load resistance is shown in figure 18. The maximum transformation factor obtained for prototype 2 is 4.1 for an input voltage of 50 mV. The least transformation factor obtained was 0.00016 for an input AC voltage of 600 mV at a load resistance of 1.5 kΩ.

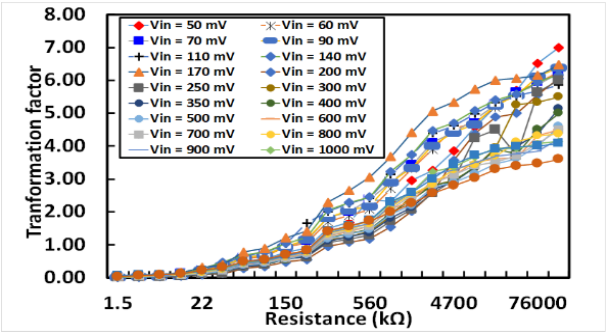

Figure 18. Transformation factor versus load resistance for prototype-2

Characterization of prototype-3

The voltage multiplier circuit prototype-3 has been tested with the same experimental setup which has been used for prototype-1 and prototype-2. The experimental data collection procedure for prototype 3 is the same as for the other three prototypes. Figure 19 shows an open circuit voltage produced by prototype 3 in response to the frequency for different input voltage signals. An input signal voltage of 75 mV to 1500 mV is generated with a function generator for the frequency range of 100 kHz to 1.5 MHz. An output open circuit DC voltage of 41.5 mV to 11280 mV is obtained for prototype-3.

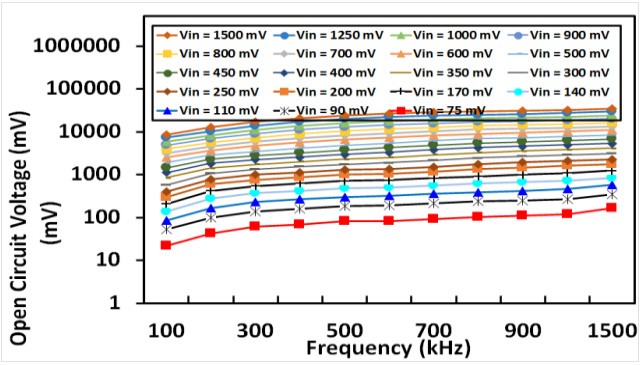

Figure 19. Output open circuit DC voltage versus input AC voltage frequency (prototype-3)

The variation of open circuit DC voltage obtained at the rectifier output in response to the input voltage is analyzed in figure 20. An input signal amplitude is varied from input 1.1 mV to 1500 mV and their corresponding DC voltage is measured. It is cleared from the figure an input AC voltage of 50 mV is converted into 350 mV DC and can achieve an output DC voltage of 7 V.

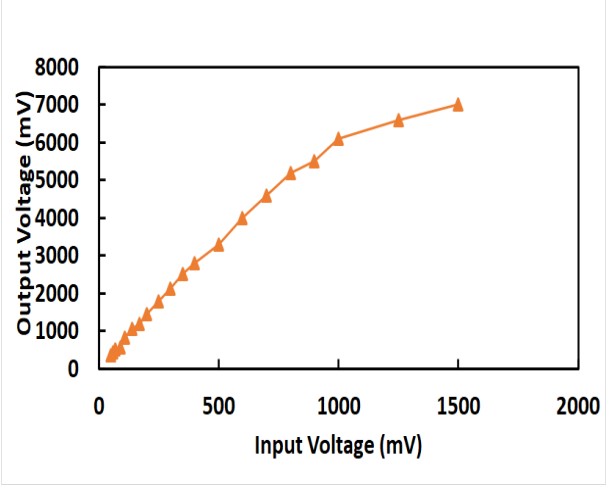

Figure 20. Output DC voltage as a function of input AC voltage for prototype 3

Figure 21 shows the Output load DC voltage produced by prototype 3 as a function of load resistance for different input voltages. During this experimentation, a series of load resistors are connected with the voltage multiplier circuit output for an input voltage ranges from 50 mV to1500 mV. It is cleared from figure 22 that the output voltage increases as the load resistance is changed from a lower value to a higher value.

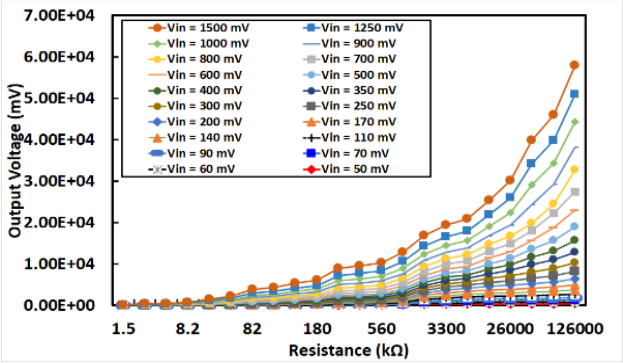

Figure 21. Output Load voltage versus load resistance (prototype 3)

Output load Power produced by prototype-3 as a function of load resistance for the different input voltage is shown in figure 22. The characterization was performed under an input frequency of 1.5 MHz. The load resistance is varied from 1.5 kΩ to 60 MΩ and the corresponding load power is recorded. At optimum load resistance of 82 kΩ, a maximum load power of 9.7 µW is produced.

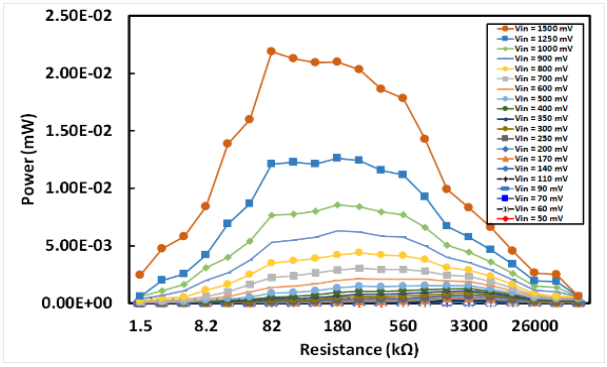

Figure 22. Load power as a function of load resistance (prototype-3)

Figure 23 shows the transformation factor (V output/V input) versus load resistance for different input voltages. The maximum transformation factor obtained is 4.1 for an input voltage of 50 mV. The least transformation factor obtained was 0.00016 for an input AC voltage of 600 mV at a load resistance of 1.5 kΩ.

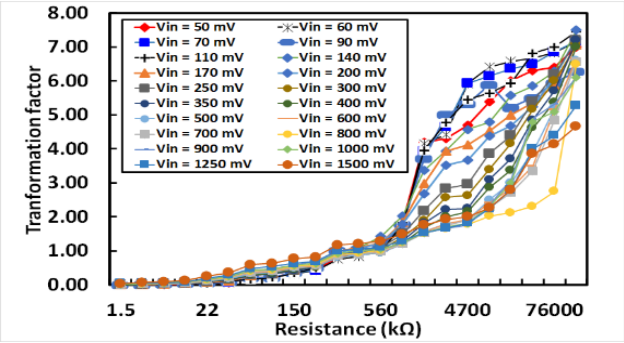

Figure 23. Transformation factor versus load resistance (Prototype-3)

Characterization of prototype-4

The block diagram and actual experimental setup used for the characterization of prototype 4 are presented in 24 and 25 respectively. It consists of flow type energy harvester developed in [XXXVI]. The harvester converts the flow energy present inside the pipeline into AC electrical signals. To convert the AC output of the harvester into DC form, the output of the harvester is connected with the voltage multiplier circuit developed in figure 7. The output of the harvester and the voltage multiplier circuit is measured and analyzed using a digital multimeter (GDM-8034, Electronic Venta) and oscilloscope (GOB-6112, Electronic Venta).

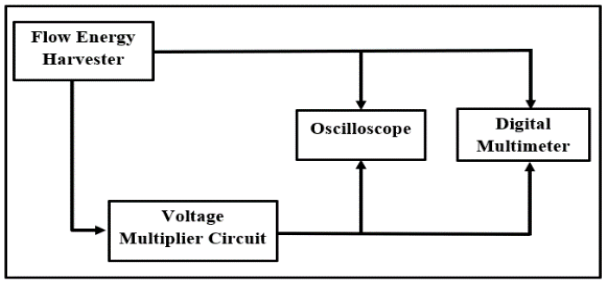

Figure 24. Block diagram of the experimental setup used for testing of prototype-4

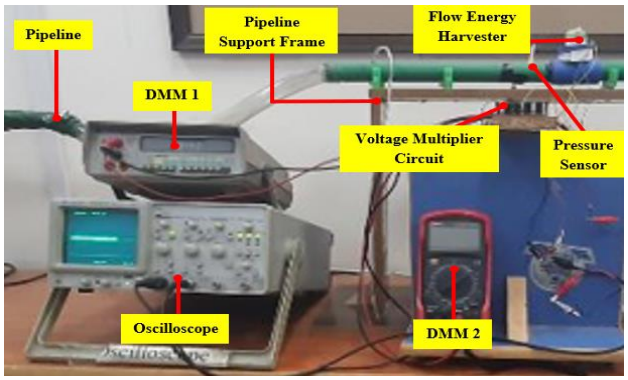

Figure 25. Developed experimental setup used for testing of prototype-4

Figure 26 and 27 shows the load AC RMS voltage produced by the harvester and the rectified load DC voltage available at the output of the voltage multiplier circuit as a function of load resistance. The output of the energy harvester and voltage multiplier circuitry is attached to a series of different resistance and their corresponding output voltage levels are measured. It is clear from this experimentation as the load resistance is varied from the lower value to the higher, the load voltage also changes from the lower to the higher value. A maximum of 354 mV load AC RMS voltage was measured across 1 kΩ of load resistance. Similarly, a maximum of 1650 mV load DC voltage is measured at the load resistance of 38 kΩ.

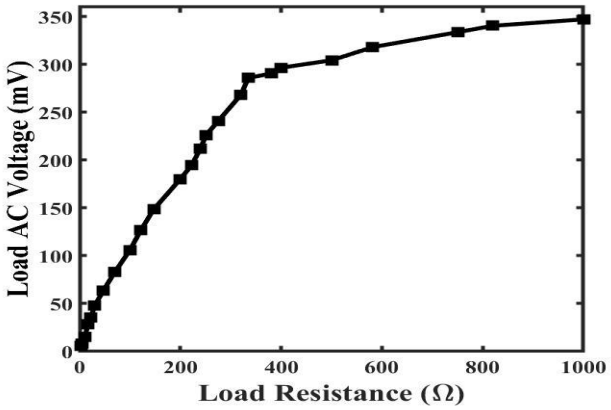

Figure 26. Load AC voltage produced by the energy harvester as a function of load resistance

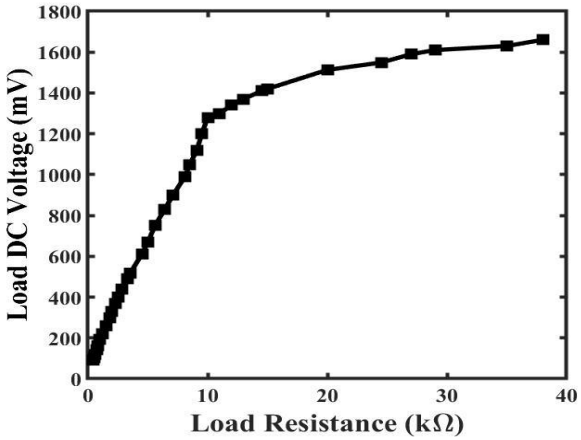

Figure 27. Load DC voltage produced by the voltage multiplier circuit as a function of load resistance

In this experimentation, the load AC power produced by the energy harvester and load DC power available at the output of the voltage multiplier circuit in response to the external load resistance is analyzed. Figure 28 shows that at the optimum load resistance of 335 Ω the maximum AC load power produced by the flow energy harvester is 244 μW. when the voltage multiplier circuit is connected with the energy

harvester, the maximum DC power produced is 164 µW at the optimum load resistance of 10 kΩ. Furthermore, it is cleared from this experimentation that the maximum load power reduced from 244 µW to 164 µW and the optimum load shifted from 335 Ω to 10 kΩ due to the internal impedance of rectifying circuitry.

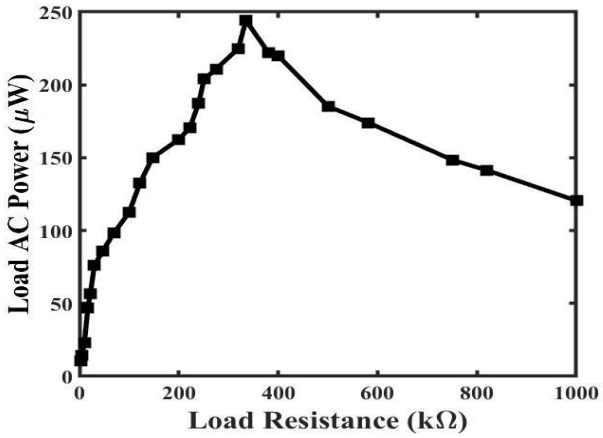

Figure 28. Load AC power produced by the energy harvester as a function of load resistance

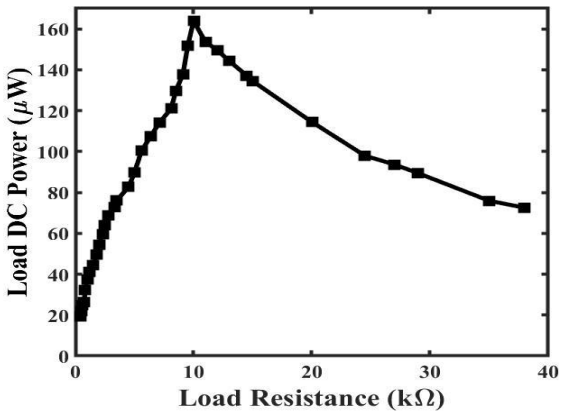

Figure 29. Load DC power produced by the voltage multiplier circuit as a function of load resistance

The summary of the developed AC to DC converter is provided in Table 2.

Table 2. Converter characterization summary

Measured parameter	Prototype-1	Prototype-2	Prototype-3	Prototype-4
Minimum AC voltage rectified	50 mV	50 mV	50 mV	50 mV
Input AC voltage range	50 mV – 1.5 V	50 mV – 1.5 V	50 mV – 1.5 V	50 mV to 5 V
Input frequency range	100 kHz – 1.5 MHz	100 kHz – 1.5 MHz	100 kHz – 1.5 MHz	100 Hz – 10 kHz
Load resistance range	1.5 kΩ – 126 MΩ	1.5 kΩ – 126 MΩ	1.5 kΩ – 126 MΩ	335 Ω – 38 kΩ
Optimum load	470 KΩ	560 KΩ	82 KΩ	10 kΩ
Maximum Power	1.1 µW	11.97 µW	9.7 µW	164 W

VI. Integration of voltage multiplier with Antenna

A patch antenna of 2.45 GHz is integrated with prototype-1, prototype-2 and prototype-3. 12 dBi transmitting antenna of 2.45 GHz is used for power transmission. Distance between the transmission antenna and rectenna is varied to see the distance impact on power. The experimental setup is shown in figure 20. The prototype-3 voltage multiplier couldn't operate because of low power and huge power losses due to seven stages. Whereas, the other two rectifiers produced power in µW.

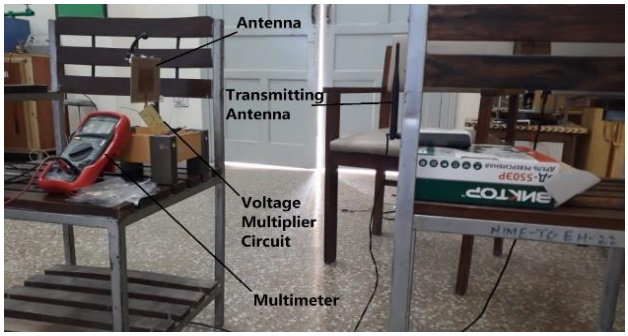

Figure 30. Experimentation setup of Rectenna testing.

As shown in Figures 21 and 22, the voltage decreases as the distance between the transmitting antenna and rectenna increases. The maximum output voltage of a rectenna achieved is 2.2 mV for prototype-1 and 3 mV for prototype-2, at 6 Inches distance and an optimum load of 126 MΩ, whereas maximum voltage at a distance of 60 Inches is 0.9 mV and 0.4 mV for prototype-1 and prototype-2 respectively, at an optimum load of 126 MΩ.

Similarly, the maximum power is attained at a minimum distance of 6 Inches. As shown in figure 23 the maximum power achieved by prototype-1 is 4.78×10^{-7} µW, at an optimum load of 4.7 MΩ. In figure 24, the voltage multiplier obtained power is 3.01×10^{-6} µW, at an optimum load of 560 kΩ, and a distance of 6 Inches. Moreover, as distance increases the power decreases and minimum power is achieved at 60 inches distance between the transmitting antenna and rectenna. Even the prototype-2 will have more power losses than prototype-1 but still, the power achieved by the prototype-2 with HSMS-285C has better performance.

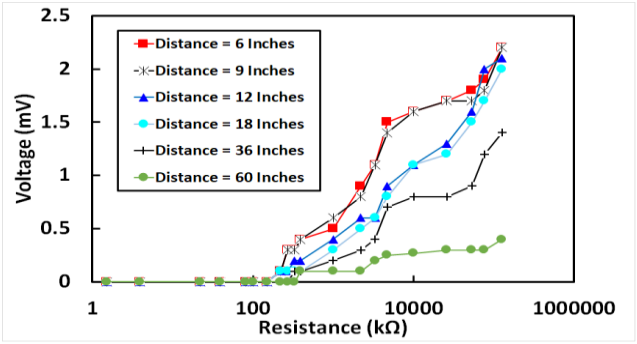

Figure 31. Two-stage Rectenna voltage versus load resistance at different distances.

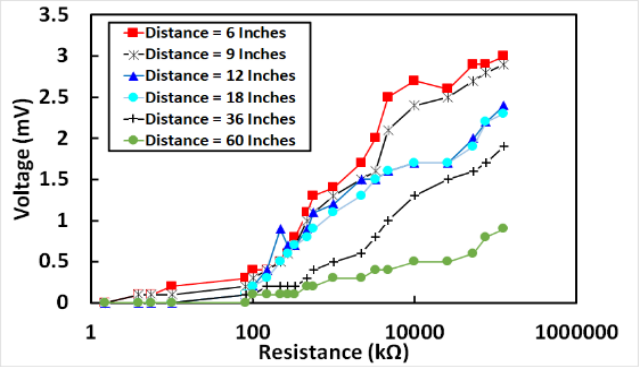

Figure 30. Three-stage Rectenna voltage versus load resistance at different distances.

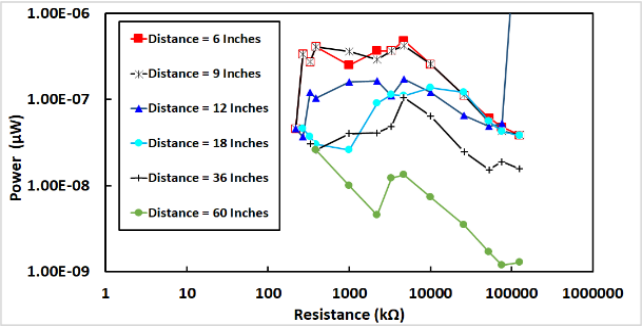

Figure 33. Two-stage Rectenna Power versus load resistance at different distances.

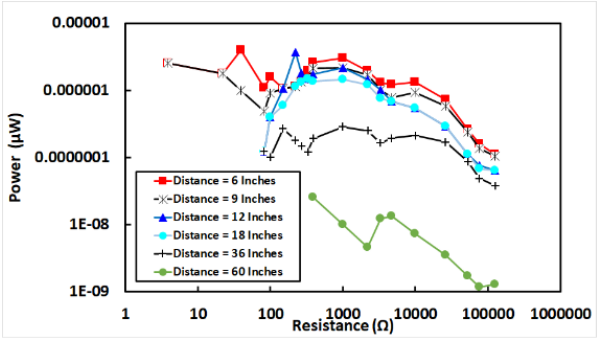

Figure 34. Three-stage Rectenna Power versus load resistance at different distances.

VII. Conclusion

The use of rectifying circuits has widespread applications. The harvested energy requires a power management circuit to power wearable/portable devices and wireless sensor nodes (WSNs). The proposed Prototype-1, Prototype-2 and prototype-3 uses commercial components and Schottky diodes and were realized on a lossy substrate. All the used elements are low-cost fabricated and especially feasible for RF energy harvesting, where the aim is to operate low power sensors and devices. Due to this, a high-scale production with minimal costs and still maintaining good performance. On a power basis, a prototype-2 circuit performed better than prototype-1 and prototype-3. The voltage multiplier circuits successfully operated at a low input voltage of 50 mV which provides its application in RF energy harvesting and vibrational energy harvesting, even at frequencies as low as 100 kHz. For maximum power transmission of 11.97 µW, at the optimum load of 560 kΩ was recorded. On integration with the antenna, the RF energy harvester produced an output power of 3.01×10^{-6} µW, at an optimum load of 560 kΩ at a frequency of 2.45 GHz.

VIII. Acknowledgement

The authors would like to acknowledge Sensors and Energy Harvesting Systems Research Lab (SEHSR Lab), Department of Mechatronics, University of Engineering and Technology, Peshawar, Pakistan.

Conflict of Interest:

There was no conflict of interest regarding this paper.

References

I. Ahmad M M, Khan F U. Review of vibration-based electromagnetic–piezoelectric hybrid energy harvesters. Int J Energy Res. 2020;1–40. https://doi.org/10.1002/er.6253

II. Ahmad MM, Khan NM, Khan FU. Review of frequency up-conversion vibration energy harvesters using impact and plucking mechanism. Int J Energy Res. 2021;1–37. https://doi.org/10.1002/er.6832

III. Akyildiz, I.F., et al., A survey on sensor networks. IEEE Communications magazine, 2002. 40(8): p. 102-114.

IV A. Leon-Masich, V. Hugo, M. B. Josep, M. Luis, and F. Freddy. High voltage led supply using a hysteretic controlled single stage boost converter. Przeglad Elektrotechniczny, vol. 88, no. 1, pp. 26–30, 2012.

V. Bibhu Prasad Ganthia, Subrat Kumar Barik, Byamakesh Nayak, : 'APPLICATION OF HYBRID FACTS DEVICES IN DFIG BASED WIND ENERGY SYSTEM FOR LVRT CAPABILITY ENHANCEMENTS'. *J. Mech. Cont.& Math. Sci., Vol.-15, No.-6, June (2020) pp 245-256*. DOI : 10.26782/jmcms.2020.06.00019

VI. Chang, Y.H. and Y.C. Chen, Multistage multiphase switched-capacitor DC–DC converter with variable-phase and PWM control. International Journal of Circuit Theory and Applications, 2012. 40(8): p. 835-857.

VII. Khan F U. A vibration based electromagnetic and piezoelectric hybrid energy harvester. Int J Energy Res. 2020;44: 6894–6916. https://doi.org/10.1002/er.5442

VIII. Khan F, Sassani F, Stoeber B. Nonlinear behaviour of membrane type electromagnetic energy harvester under harmonic and random vibrations. Microsyst. Technol. 2014;20:1323-1335. http://doi.org/10.1007/s00542-013-1938-1.

IX. Khan F U, Qadir M U. State-of-the-art in vibration-based electrostatic energy harvesting. J Micromech Microeng. 2016;26:103001.

X. Khan FU, Khattak MU. Contributed Review: Recent developments in acoustic energy harvesting for autonomous wireless sensor nodes applications. Rev. Sci. Instrum. 2016;87:021501. http://doi.org/10.1063/1.4942102.

XI. Ehab Belal, Hassan Mostafa, Yehea Ismail and M. Sameh Said. A Voltage Multiplying AC/DC Converter for Energy Harvesting Applications.

XII. E. M. Ali, N. Z. Yahaya, N. Perumal, M. A. Zakariya. Development of Cockcroft-Walton voltage multiplier for RF energy harvesting applications. Journal of Scientific Research and Development 3 (3): 47-51, 2016.

XIII. E. M. Ali, N. Z. Yahaya, N. Perumal and M. A. Zakariya. DESIGN AND DEVELOPMENT OF HARVESTER RECTENNA AT GSM BAND FOR BATTERY CHARGING APPLICATIONS. Journal of Engineering and Applied Sciences VOL. 10, NO 21, NOVEMBER, 2015.

XIV. Filiz SARI, Yunus UZUN. A COMPARATIVE STUDY: VOLTAGE MULTIPLIERS FOR RF ENERGY HARVESTING SYSTEM. Commun.Fac.Sci.Univ.Ank.Series A2-A3 Volume 61, Number 1, Pages 12-23 2019.

XV. Farid Khan, Farrokh Sassani and Boris Stoeber Copper foil-type vibration-based electromagnetic energy harvester 2010 J. Micromech. Microeng. 20 125006. https://doi.org/10.1088/0960-1317/20/12/125006

XVI. Hagerty, J.A., et al., Recycling ambient microwave energy with broad-band rectenna arrays. IEEE Transactions on Microwave Theory and Techniques, 2004. 52(3): p. 1014-1024.

XVII. Hamayun Khan, Sheeraz Ahmed, Rehan Ali Khan, S. Arhan Haider Shah, Zeeshan Najam, Hasnain Abbas, Asif Nawaz, Zubair Aslam Khan, : AN IOT BASED ENERGY OPTIMIZATION TECHNIQUE FOR ELECTRICAL EQUIPMENT'S USING WIRELESS SENSOR NETWORKS. J. Mech. Cont. & Math. Sci., Vol.-15, No.-8, August (2020) pp 628-646. DOI : 10.26782/jmcms.2020.08.00053

XVIII. Jia, J. and K.N. Leung, Improved active-diode circuit used in voltage doubler. International Journal of Circuit Theory and Applications, 2012. 40(2): p. 165-173.

XIX. J. Zakis, D. Vinnikov, I. Roasto, and R. Strzelecki. Design guidelines of new step-up DC/DC converter for fuel cell powered distributed generation systems," in Proceedings of the 8th International Symposium on Topical Problems in the Field of Electrical and Power Engineering, pp. 33–41, Parnu, Estonia, January 2010.

XX. Kavuri Kasi Annapurna Devi, Norashidah Md. Din, Chandan Kumar Chakrabarty. Optimization of the Voltage Doubler Stages in an RF-DC Convertor Module for Energy Harvesting. Circuits and Systems, 2012, 3, 216-222.

XXI. Khan, F.U.; Ahmad, S. Flow type electromagnetic based energy harvester for pipeline health monitoring system. Energy Convers. Manag. 2019, 200, 112089. https://doi.org/10.1016/j.enconman.2019.112089

XXII. Khan FU. Review of non-resonant vibration based energy harvesters for wireless sensor nodes. J Renewable Sustainable Energy. 2016;8:044702. http://doi.org/10.1063/1.4961370.

XXIII. Khajuria, R. and S. Gupta. Energy optimization and lifetime enhancement techniques in wireless sensor networks: A survey. in International Conference on Computing, Communication & Automation. 2015. IEEE.

XXIV. Muhammad Iqbal, Farid Ullah Khan. Hybrid vibration and wind energy harvesting using combined piezoelectric and electromagnetic conversion for bridge health monitoring applications. Energy Conversion and Management 2018 Vol. 172, Pages 611-618. https://doi.org/10.1016/j.enconman.2018.07.044

XXV. Makowski, M.S. and D. Maksimovic. Performance limits of switched-capacitor DC-DC converters. in Proceedings of PESC'95-Power Electronics Specialist Conference. 1995. IEEE.

XXVI. Mitcheson, P.D., et al., Architectures for vibration-driven micropower generators. Journal of microelectromechanical systems, 2004. 13(3): p. 429-440.

XXVII. N. M. Din, C. K. Chakrabarty, A. Bin Ismail, K. K. A. Devi, and W.-Y. Chen. DESIGN OF RF ENERGY HARVESTING SYSTEM FOR ENERGIZING LOW POWER DEVICES. Progress In Electromagnetics Research, Vol. 132, 49–69, 2012 .

XXVIII. Pillai, M.A. and E. Deenadayalan, A review of acoustic energy harvesting. International journal of precision engineering and manufacturing, 2014. 15(5): p. 949-965.

XXIX. Sakai, Y., et al., Highly efficient pulsed power supply system with a two-stage LC generator and a step-up transformer for fast capillary discharge soft x-ray laser at shorter wavelength. Review of Scientific Instruments, 2010. 81(1): p. 013303.

XXX. Samuel S. B. Hong, Rosdiazli Ibrahim, Mohd H. Md. Khir, Mohammad A. Zakariya, and Hanita Daud. WI-FI ENERGY HARVESTER FOR LOW POWER RFID APPLICATION. Progress In Electromagnetics Research C, Vol. 40, 69–81, 2013.

XXXI. Shaikh, F.K., S. Zeadally, and E. Exposito, Enabling technologies for green internet of things. IEEE Systems Journal, 2015. 11(2): p. 983-994.

XXXII. Shenck, N.S. and J.A. Paradiso, Energy scavenging with shoe-mounted piezoelectrics. IEEE micro, 2001. 21(3): p. 30-42.

XXXIII. Po-Hung Chen, Koichi Ishida, Xin Zhang, Yasuaki Okuma, Yoshikatsu Ryu, Makoto Takamiya, and Takayasu Sakurai. 0.18-V Input Charge Pump with Forward Body Biasing in Startup Circuit using 65nm CMOS. Proc. IEEE Custom Integrated Circuits Conf. (CICC), 2010.

XXXIV. Tuna, G., et al., Energy harvesting techniques for industrial wireless sensor networks. inIndustrial Wireless Sensor Networks: Applications, Protocols, Standards, and Products, GP Hancke and VC Gungor, Eds, 2017: p. 119-136.

XXXV. T. Meng, H. Ben, D. Wang, and H. Huang. Starting strategies of three-phase single-stage PFC converter based on isolated fullbridge boost topology. Przeglad Elektrotechniczny, vol. 87, no. 3, pp. 281–285, 2011.

XXXVi. Vandana Niranjan, Maneesha Gupta. Low voltage four-quadrant analog multiplier using dynamic threshold MOS transistors. Microelectronics International Volume 26 · Number 1 · 2009 · 47–52.

XXXVII. W. U. Rahman and F. U. Khan, "Modeling and Simulation of Flow-Based Circular Plate Type Piezoelectric Energy Harvester for Pipeline's Monitoring," 2019 22nd International Multitopic Conference (INMIC), 2019, pp. 1-6, doi: 10.1109/INMIC48123.2019.9022755.

XXXVIII. W. Li, X. Xiang, C. Li, and X. He. Interleaved high step-up ZVT converter with built-in transformer voltage doubler cell for distributed PV generation system. IEEE Transactions on Power Electronics, vol. 28, no. 1, pp. 300–313, 2013.

XXXIX. Weiser, M., The Computer for the 21 st Century. Scientific American, 1991. 265(3): p. 94-105.

XL. Y.C. Wong, P.C. Tan, M. M. Ibrahim, A.R. Syafeeza, N. A. Hamid. Dickson Charge Pump Rectifier using Ultra-Low Power (ULP) Diode for BAN Applications. Journal of Telecommunication, Electronic and Computer Engineering Vol. 8 No. 9 September – December 2016.